

**Supporting Information for**  
**Molecular effects of Familial Hypertrophic Cardiomyopathy-**  
**related mutations in the TNT1 domain of cTnT**

Edward P. Manning,<sup>†</sup> Jil C. Tardiff,<sup>‡,§</sup> Steven D. Schwartz<sup>\*,†,⊥,||</sup>

*Dept of Biophysics, Albert Einstein College of Medicine, 1300 Morris Park Ave, Bronx, NY  
10461, Dept of Medicine, University of Arizona, Tucson, AZ 85724, Dept of Cellular and  
Molecular Medicine, University of Arizona, Tucson, AZ 85724, Dept of Biochemistry, Albert  
Einstein College of Medicine, Bronx, NY 10461, and Dept of Chemistry, 306 East University  
Blvd, University of Arizona, Tucson, AZ 85721*

E-mail: sschwartz@aecom.yu.edu

Phone: (718) 430-2139. Fax: (718) 430-8819

---

<sup>\*</sup>To whom correspondence should be addressed

<sup>†</sup>Department of Biophysics

<sup>‡</sup>Department of Medicine

<sup>§</sup>Department of Cellular and Molecular Medicine

<sup>⊥</sup>Department of Biochemistry

<sup>||</sup>Department of Chemistry

## Components of complete cTn model

Compilation of known and predicted structures of cTn complex. This reflects the inclusion of PDB ID 2JPW and 1Y TZ into our existing model.<sup>33</sup>

\*= 137-147 in cTnI of PDB entry 1J1E is homologous to 104-114 in sTnI of PDB entry 1Y TZ.

cTn subunit (Accession number)	Structural Source (by Residue Number)			PSIPRED
	PDB 1J1E (chain ID)	PDB 2JPW (Model No.)	PDB 1Y TZ (chain ID)	
cTnT (X74819; 288 rr.)	---	---	---	1-201
	202-276	---	---	---
	---	---	---	277-288
	(chain E)	---	---	---
cTnI (M64247; 210 rr.)	---	1-31	---	---
	---	---	---	32-39
	40-136	---	---	---
	---	---	137-147*	---
	148-191	---	---	---
	---	---	---	192-210
	(chain F)	(Model 1)	(chain I)	---
cTnC (NM_003280; 161 rr.)	1-48	---	---	---
	---	---	---	49-50
	51-161	---	---	---
	(chain D)	---	---	---

## Substitutions to contributing structures

Changes made to PDB ID 2JPW and 1Y TZ in order for primary sequences to comply with human cTn.

Destination in hcTnI	Structural Source	Changes Made
1-31	res. 1-32 PDB 2JPW	res. 4: E to G res. 10: G to R res. 13: Q to R res. 19: V to I res. 25: A deleted
137-147	res. 104-114 PDB 1Y TZ	res. 110: P to T

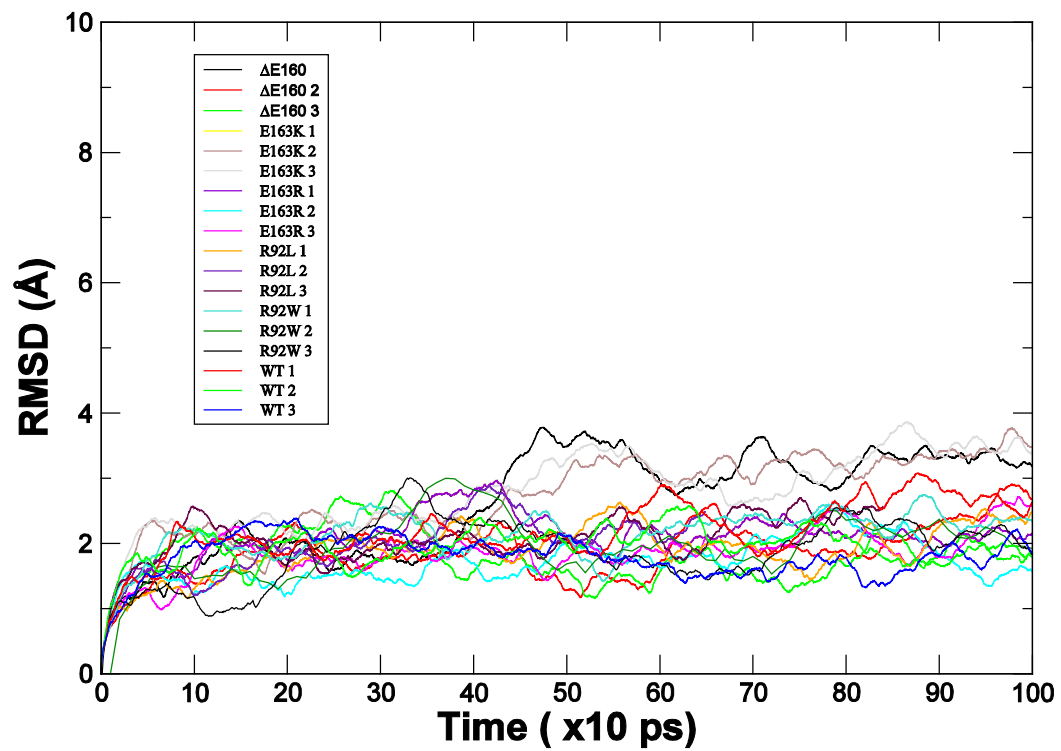
## Rmsd data

Average rmsd (rounded to nearest Å) for the 1 ns production runs

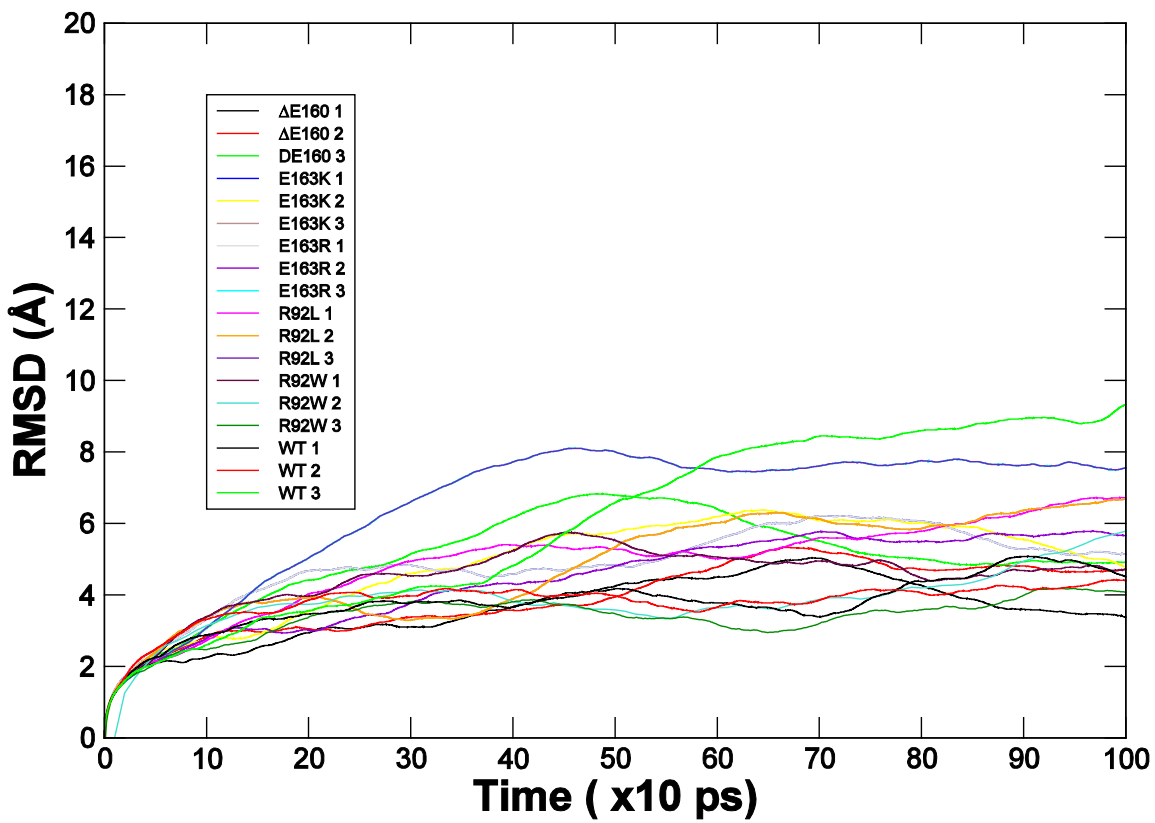
cTnT variant	TNT1	cTn core
WT	2, 2, 2	4, 4, 6
R92L	2, 2, 2	5, 4, 5
R92W	2, 2, 2	5, 6, 4
$\Delta$ E160	2, 2, 2	5, 4, 4
E163K	3, 3, 3	7, 6, 5
E163R	2, 2, 2	5, 4, 7

We analyzed the stability of our molecules by measuring the rmsd of TNT1 (residues 70-170 cTnT) and the core of cTn (residues 205-288 cTnT, all of cTnC, and 1-159 of cTnI) with respect to their minimized structures. We eliminated hypervariable regions of cTnT<sup>25</sup> and cTnI<sup>29,30</sup> whose fluctuations appear critical to signal transduction but less important for structural stability. The rmsd as a function of time for our simulations quickly steadied for TNT1 and the cTn core, ranging from two to three Å for TNT1 and four to seven Å for the cTn core, as noted in the table above. The graphs for each are included below. We ensured that rgyr measurements for TNT1 were measured only once the region was structurally stable.

# RMSD of TNT1



## RMSD of cTn core



## Calcium coordination data

Data for Figure 5. Coordinating oxygens interacting with calcium were based on analysis of WT simulations. No new interactions between site II atoms and calcium occurred during the course of any WT or mutant simulations.

	65 OD2	69 OG	71 O	76 OE1	76 OE2
<u>Average</u>					
WT	3.5	4.7	3.1	3.0	3.0
$\Delta$ E160	2.5	3.1	2.7	2.8	2.7
E163K	5.3	6.6	3.6	4.9	4.3
E163R	3.9	5.6	3.3	3.1	3.0
<u>Sim1</u>					
WT	2.53	3.06	2.70	2.86	2.64
$\Delta$ E160	2.60	3.61	2.70	2.82	2.72
E163K	4.94	7.34	4.02	4.14	2.60
E163R	4.20	5.19	2.71	3.66	3.01
<u>Sim 2</u>					
WT	2.55	4.50	2.67	2.81	2.69
$\Delta$ E160	2.51	2.81	2.70	2.78	2.65
E163K	2.59	2.78	2.68	3.48	2.98
E163R	2.55	4.90	3.31	2.81	2.90
<u>Sim 3</u>					
WT	5.47	6.67	4.07	3.40	3.51
$\Delta$ E160	2.50	2.80	2.71	2.76	2.69
E163K	8.44	9.64	5.84	7.17	7.31
E163R	4.06	6.70	4.10	2.83	2.91

We performed three separate 1 ns simulations with varying initial conditions for WT and each mutant and took the average distances of the oxygens that interact with calcium in site II (residues 54-90) of cTnC. By subtracting the mutant distances from the WT, we see the average change in distances between the interacting oxygens and calcium. These values are graphed in Figure 5. A positive difference means that the distance between the mutant oxygen and calcium has decreased, and vice versa. We can see that the distances for  $\Delta$ E160 tend to decrease, while the distances for E163K and E163R tend to increase. This implies that once calcium is bound to site II cTnC of  $\Delta$ E160, it is less likely to leave than if calcium were bound to WT. The opposite is true for E163K and E163R; it is more likely that calcium bound to site II of E163K and

E163R will dissociate than if it were bound to WT. Therefore, more calcium would be required to activate the thin filaments of E163K and E163R than WT while less would be required for the same degree of activation of  $\Delta$ E160 mutants than WT. This directly corresponds to preliminary data of calcium-sensitivity where E163K and E163R were found to decrease calcium-sensitivity and  $\Delta$ E160 was found to increase calcium sensitivity with respect to WT.<sup>51</sup>



## Rgyr and R-IVM data

Data for Figures 3 and 7

	EC <sub>50</sub>	<i>n</i> , Hill coefficient	Flexibility: (range)
WT(54)	7.08 ± 0.020	1.80 ± 0.10	0.056 (0.041 - 0.085)
R92L	7.02 ± 0.010	1.20 ± 0.40	0.071 (0.051 - 0.084)
R92W	6.90 ± 0.010	1.50 ± 0.50	0.067 (0.051 - 0.195)
WT(18)	7.58 ± 0.001	2.62 ± 0.04	0.057 (0.041 - 0.085)
ΔE160	7.99 ± 0.020	2.37 ± 0.11	0.042 (0.027 - 0.057)
E163K	7.28 ± 0.002	1.58 ± 0.01	0.085 (0.063 - 0.290)
E163R	6.93 ± 0.010	1.64 ± 0.04	0.067 (0.047 - 0.075)

WT(54) represents R-IVM data collected at high ionic strength.<sup>26</sup> WT(18) represents R-IVM data collected at low ionic strength.<sup>51</sup> Flexibility is reflected by the variance ( $\sigma^2$ ) of the rgyr. Data for the flexibility of all three trajectories are shown. A Pearson correlation was performed to determine the general relationship between flexibility and calcium properties measured by R-IVM. It should be noted that a Pearson correlation assumes a linear relationship. Due to the limited amount of data points, the possibility of a non-linear relationship cannot be excluded.

## Site II E-F hand sequence alignment

Alignment and assignment of canonical E-F hand positions to site II cTnC.

E-F hand position				1		3		5		7		<u>9</u>		12			
Residue number	62	63	64	65	66	67	68	69	70	71	72	73	74	75	76	77	78
Residue name	D	E	V	D	E	D	G	S	G	T	V	D	F	D	E	F	L

A canonical E-F hand has seven oxygen-calcium interactions resulting from six residues at positions 1, 3, 5, 7, 9, and 12. Underlined numbers indicate residues that require water bridges to mediate oxygen-calcium interactions. Due to the implicit solvation of our model these interactions cannot be accurately simulated.

## Secondary structural changes

Secondary structure analysis of mutations resulting in common pathway of TNT1 mutationally-induced changes throughout cTn. Sequences for WT and mutants ΔE160, E163K, E163R, R92L, and R92W are aligned for each subunit of cTn.

### cTnC structural changes

```

1
161
WT  MDITYAAVQLTTEQKHEFAAFDFVYLGAEDGSIKTELQKWNMLGNQPTPEELQNTIDVDEDCSGTVDVDFEFLWVWVRSKCDGSKSESEELSDLFNMFQDNADGYDLEELKIMLQATGETITEDDIEELMKGDKNDGRLDYCEFLFPEYQVE
4160E MDITYAAVQLTTEQKHEFAAFDFVYLGAEDGSIKTELQKWNMLGNQPTPEELQNTIDVDEDCSGTVDVDFEFLWVWVRSKCDGSKSESEELSDLFNMFQDNADGYDLEELKIMLQATGETITEDDIEELMKGDKNDGRLDYCEFLFPEYQVE
E163K MDITYAAVQLTTEQKHEFAAFDFVYLGAEDGSIKTELQKWNMLGNQPTPEELQNTIDVDEDCSGTVDVDFEFLWVWVRSKCDGSKSESEELSDLFNMFQDNADGYDLEELKIMLQATGETITEDDIEELMKGDKNDGRLDYCEFLFPEYQVE
E163R MDITYAAVQLTTEQKHEFAAFDFVYLGAEDGSIKTELQKWNMLGNQPTPEELQNTIDVDEDCSGTVDVDFEFLWVWVRSKCDGSKSESEELSDLFNMFQDNADGYDLEELKIMLQATGETITEDDIEELMKGDKNDGRLDYCEFLFPEYQVE
R92L MDITYAAVQLTTEQKHEFAAFDFVYLGAEDGSIKTELQKWNMLGNQPTPEELQNTIDVDEDCSGTVDVDFEFLWVWVRSKCDGSKSESEELSDLFNMFQDNADGYDLEELKIMLQATGETITEDDIEELMKGDKNDGRLDYCEFLFPEYQVE
R92W MDITYAAVQLTTEQKHEFAAFDFVYLGAEDGSIKTELQKWNMLGNQPTPEELQNTIDVDEDCSGTVDVDFEFLWVWVRSKCDGSKSESEELSDLFNMFQDNADGYDLEELKIMLQATGETITEDDIEELMKGDKNDGRLDYCEFLFPEYQVE
|-----Site I-----| |-----Site II-----| |-----Site III-----| |-----Site IV-----|

```

### cTnI structural changes

```

1
810
WT  MADQSSDARPEPAPPIRRSSNYTAYATEPHAKKSKISASRKLQKTLILQIAKQLEKEAEERKGEKGRALSTRAQPLELGLQFAELQDLARQLHARVDVDEERYDIEAVYKNTIETIDLTKIFLQAGFQPTLAVRISADANQALLGARAKESLDLAHLQYKKEDEKENREYQVQWKNIDALSGHGRKQKQFES
4160E MADQSSDARPEPAPPIRRSSNYTAYATEPHAKKSKISASRKLQKTLILQIAKQLEKEAEERKGEKGRALSTRAQPLELGLQFAELQDLARQLHARVDVDEERYDIEAVYKNTIETIDLTKIFLQAGFQPTLAVRISADANQALLGARAKESLDLAHLQYKKEDEKENREYQVQWKNIDALSGHGRKQKQFES
E163K MADQSSDARPEPAPPIRRSSNYTAYATEPHAKKSKISASRKLQKTLILQIAKQLEKEAEERKGEKGRALSTRAQPLELGLQFAELQDLARQLHARVDVDEERYDIEAVYKNTIETIDLTKIFLQAGFQPTLAVRISADANQALLGARAKESLDLAHLQYKKEDEKENREYQVQWKNIDALSGHGRKQKQFES
E163R MADQSSDARPEPAPPIRRSSNYTAYATEPHAKKSKISASRKLQKTLILQIAKQLEKEAEERKGEKGRALSTRAQPLELGLQFAELQDLARQLHARVDVDEERYDIEAVYKNTIETIDLTKIFLQAGFQPTLAVRISADANQALLGARAKESLDLAHLQYKKEDEKENREYQVQWKNIDALSGHGRKQKQFES
R92L MADQSSDARPEPAPPIRRSSNYTAYATEPHAKKSKISASRKLQKTLILQIAKQLEKEAEERKGEKGRALSTRAQPLELGLQFAELQDLARQLHARVDVDEERYDIEAVYKNTIETIDLTKIFLQAGFQPTLAVRISADANQALLGARAKESLDLAHLQYKKEDEKENREYQVQWKNIDALSGHGRKQKQFES
R92W MADQSSDARPEPAPPIRRSSNYTAYATEPHAKKSKISASRKLQKTLILQIAKQLEKEAEERKGEKGRALSTRAQPLELGLQFAELQDLARQLHARVDVDEERYDIEAVYKNTIETIDLTKIFLQAGFQPTLAVRISADANQALLGARAKESLDLAHLQYKKEDEKENREYQVQWKNIDALSGHGRKQKQFES
|-----non-regulatory domain-----| |-----IT arm-----| |-----inhib-| |-----switch pep-| |-----mobile domain-----| |-----regulatory domain-----|
** -- site of beta-adrenergic phosphorylation site

```

### cTnT structural changes

```

1
280
WT  MSDIEEVYEEYEEQEEAAVEEQEAAEDDAEAEAEETEAEEDEEEEAKEAEDGPEESKPKPSFPHPLVPPKIPQGERVDFDIHQKMEKDLNELQALTEAFENKQKEEELVSLKDRLENRAAERAQQRINERKEKQKQ
4160E MSDIEEVYEEYEEQEEAAVEEQEAAEDDAEAEAEETEAEEDEEEEAKEAEDGPEESKPKPSFPHPLVPPKIPQGERVDFDIHQKMEKDLNELQALTEAFENKQKEEELVSLKDRLENRAAERAQQRINERKEKQKQ
E163K MSDIEEVYEEYEEQEEAAVEEQEAAEDDAEAEAEETEAEEDEEEEAKEAEDGPEESKPKPSFPHPLVPPKIPQGERVDFDIHQKMEKDLNELQALTEAFENKQKEEELVSLKDRLENRAAERAQQRINERKEKQKQ
E163R MSDIEEVYEEYEEQEEAAVEEQEAAEDDAEAEAEETEAEEDEEEEAKEAEDGPEESKPKPSFPHPLVPPKIPQGERVDFDIHQKMEKDLNELQALTEAFENKQKEEELVSLKDRLENRAAERAQQRINERKEKQKQ
R92L MSDIEEVYEEYEEQEEAAVEEQEAAEDDAEAEAEETEAEEDEEEEAKEAEDGPEESKPKPSFPHPLVPPKIPQGERVDFDIHQKMEKDLNELQALTEAFENKQKEEELVSLKDRLENRAAERAQQRINERKEKQKQ
R92W MSDIEEVYEEYEEQEEAAVEEQEAAEDDAEAEAEETEAEEDEEEEAKEAEDGPEESKPKPSFPHPLVPPKIPQGERVDFDIHQKMEKDLNELQALTEAFENKQKEEELVSLKDRLENRAAERAQQRINERKEKQKQ
|-----PDB 225H cTnTnTnTn-----|
|-----IT arm-----|
|-----TNT1-TNT2 linker region-----|

```

This analysis represents the data for Figure 9. Each line represents the average change in secondary structure per residue over the three simulations of that particular variant. The mutation site for each variant is underlined. Residue letters are colored as a function of their average change in secondary structure with respect to WT. Black = no change; red = decrease in secondary structure; green = increase in secondary structure. 100 ps snapshots of cTn were taken during each simulation. These snapshots were aligned by their respective residues and compared with WT. A change in secondary structure was defined as a 33% or greater difference in the structural sample for each residue.